AD-A074 108 MICHIGAN STATE UNIV EAST LANSING ULTRASONICS LAB F/G 20/1
OPTICAL METHODS FOR ABSOLUTE MEASUREMENT OF SOUND PRESSURE IN L--ETC(U)
JUL 62 E A HIEDEMANN NONR-2587(01)
UNCLASSIFIED TR-6 NL

| OF |

ADA
074108

END
DATE
FILMED
10-79
DDC

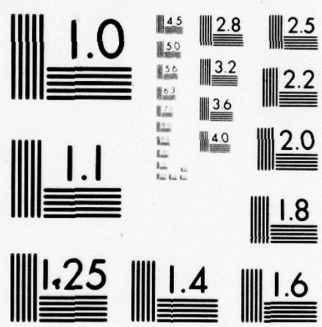

MICROCOPY RESOLUTION TEST CHART

LEVEL

Dr.

A074112

MICHIGAN STATE UNIVERSITY

PHYSICS DEPARTMENT

ULTRASONICS LABORATORY

Office of Naval Research
Contract Nonr-2587(01)
Project No. NR 385-425

OPTICAL METHODS FOR ABSOLUTE MEASUREMENT OF SOUND PRESSURE IN LIQUIDS.

Technical Report No. 6.

E. A. Hiedemann
Main Investigator

July 1962

UNCLASSIFIED

SECURITY CLASSIFICATION OF THIS PAGE (When Data Entered)

REPORT DOCUMENTATION PAGE		READ INSTRUCTIONS BEFORE COMPLETING FORM
1. REPORT NUMBER No. 6	2. GOVT ACCESSION NO.	3. RECIPIENT'S CATALOG NUMBER
4. TITLE (and Subtitle) (6) OPTICAL METHODS FOR ABSOLUTE MEASUREMENT OF SOUND PRESSURE IN LIQUIDS.		5. TYPE OF REPORT & PERIOD COVERED 6. PERFORMING ORG. REPORT NUMBER
7. AUTHOR(s) [redacted] (10) E. A. / Hiedemann		8. CONTRACT OR GRANT NUMBER(s) (15) Nonr-2587(01)
9. PERFORMING ORGANIZATION NAME AND ADDRESS Michigan State University Physics Dept, Ultrasonics Lab East Lansing, MI		10. PROGRAM ELEMENT, PROJECT, TASK AREA & WORK UNIT NUMBERS NR 385-425
11. CONTROLLING OFFICE NAME AND ADDRESS Office of Naval Research, Code 220 800 North Quincy Street Arlington, VA 22217		12. REPORT DATE (11) JUL [redacted]62 13. NUMBER OF PAGES
14. MONITORING AGENCY NAME & ADDRESS (if different from Controlling Office) (9) Technical rept.,		15. SECURITY CLASS. (of this report) UNCLAS 15a. DECLASSIFICATION/DOWNGRADING SCHEDULE

16. DISTRIBUTION STATEMENT (of this Report)

Approved for public release; distribution unlimited.

17. DISTRIBUTION STATEMENT (of the abstract entered in Block 20, if different from Report)

(14) TR-6 (12) 35p.

18. SUPPLEMENTARY NOTES

19. KEY WORDS (Continue on reverse side if necessary and identify by block number)

20. ABSTRACT (Continue on reverse side if necessary and identify by block number)

355 850

DD FORM 1 JAN 73 1473 EDITION OF 1 NOV 65 IS OBSOLETE

S/N 0102-LF-014-6601

UNCLASSIFIED

This Technical Report consists of papers published between January and June, 1962 by the staff and graduate students supported by the Office of Naval Research.

<u>Staff</u>:

E. A. Hiedemann	Professor of Physics (Research)
M. A. Breazeale	Assistant Professor (Research)
W. G. Mayer	Assistant Professor (Research)
L. E. Hargrove	Research Associate
D. Bradley	Graduate Research Assistant
B. D. Cook	Graduate Research Assistant
W. R. Klein	Graduate Research Assistant
W. W. Lester	Graduate Research Assistant

TABLE OF CONTENTS

NUMERICAL CALCULATIONS OF MERTEN'S CORRECTION FOR ZERO AND FIRST ORDERS

by

Bill D. Cook

The simplified theory of Raman and Nath for the diffraction of light by ultrasonic waves is valid only for a small range of experimental values. Mertens[1] has supposedly extended this range by a perturbation method. It is the purpose of this memorandum to give certain numerical values which will allow the computation of the light intensities in the zero and first diffracted orders from Merten's results.

The results of Mertens for the light amplitude of the nth order can be expressed as

$$\phi_n = J_n(v) + i\,H\,A_n(v) + H^2 B_n(v) \tag{1}$$

where $J_n(v)$ is the nth order Bessel function of argument v. The parameter H is $\frac{2\lambda\,\pi\,L}{\mu_o \lambda^{*2}}$ where λ is the wavelength of light, L is the path length of the light through the ultrasonic beam, μ_o is the index of refraction of the undisturbed medium, and λ^* is the wavelength of sound[2]. $A_n(v)$ and $B_n(v)$ are power series expressed as follows

$$A_n = \sum_{m=0}^{\infty} a_{n,m}\, v^{2m+n} \tag{2}$$

and

$$B_n = \sum_{m=1}^{\infty}{}' \, b_{n,m}\, v^{2m+n-2} \tag{3}$$

where

$$a_{n,m} = \frac{(-1)^m\,[2m+n(2n+1)]}{6\,(2^{2m+n+1})\,(m!)(m+n)!} \tag{4}$$

and $$b_{n,m} = \frac{(-1)^m\,[6m + (n+1)(10n-7)]\,[m + 1/6(2n^2 + 3n-6)]}{(60)\,(2^{2m+n})(m-1)!\,(m+n-1)!} \qquad (5)$$

The prime over the summation sign in Eq. (3) means that the sum starts with $m = 2$ when $n = 0$. The light intensity is given by

$$I_n = \phi_n\,\phi_n^* = \qquad (6)$$

$$J_n^2(v) + H^2\,(A_n^2(v) + 2J_n\,B_n(v)\,) + H^4\,B_n^2\,(v) = \qquad (7)$$

$$J_n^2(v) + H^2\,G_n(v) + H^4\,B_n^2\,(v),$$

where $G_n(v) = A_n^2(v) + 2J_nB_n(v)$ (8)

Mertens gives only the first two terms of Eq. (8) in his final result. Tables I and II give numerical values needed to compute I_o and I_1 respectively, from equation (8).

The parameter H is completely determined by the experimental condition. For water and the Hg green line, it can be expressed as

$$H = 1.5 \times 10^{-2}\,F^2L \qquad (9)$$

where F is the frequency in megacycles and L is the width of the sound beam in cm.

Table III gives the values of the $a_{n,m}$ and $b_{n,m}$ in order that one may calculate A_n and B_n for any value of v.

	TABLE I		TABLE II	
	I	II	I	II
v	$G_o(v)$	B_o^2	$G_1(v)$	B_1^2
0.2	.000411	-	-.00201	.000017
0.4	.001574	-	-.000717	.000061
0.6	.003295	.000003	-.001306	.000114
0.8	.005894	.000008	-.001262	.000156
1.0	.007260	.000015	-.001311	.000168
1.2	.008918	.000023	-.000053	.001415
1.4	.010078	.000029	.002318	.000086
1.6	.010680	.000029	.005777	.000027
1.8	.010807	.000022	.010095	-
2.0	.010669	.000010	.014855	.000043
2.2	.010653	-	.019520	.000184
2.4	.010697	.000006	.023517	.000431
2.6	.011691	.000044	.026343	.000763
2.8	.013378	.000131	.027660	.001133
3.0	.015895	.000280	.027366	.001472
3.2	.019095	.000494	.025630	.001705
3.4	.022680	.000761	.022877	.001771
3.6	.026245	.001053	.019730	.001636
3.8	.029348	.001327	.016909	.001315
4.0	.031593	.001534	.015113	.000872
4.2	.032707	.001624	.014898	.000415
4.4	.032603	.001564	.016573	.000083
4.6	.031410	.001347	.020137	.000014
4.8	.029465	.001000	.025287	.000316
5.0	.027269	.000592	.031354	.001038
5.2	.025404	.000222	.037605	.002142
5.4	.024443	.000013	.043166	.003511
5.6	.024846	.000087	.047262	.004947
5.8	.026880	.000545	.049339	.006205
6.0	.030572	.001440	.049161	.007040
6.2	.035253	.002650	.047068	.007326
6.4	.040874	.004187	.043270	.006879
6.6	.046559	.005826	.038682	.005775
6.8	.051561	.007332	.034261	.004198
7.0	.055202	.008458	.030973	.002459
7.2	.057001	.008985	.029614	.000952
7.4	.056756	.008772	.030706	.000086
7.6	.054604	.007798	.034356	.000205
7.8	.051008	.006184	.040250	.001513
8.0	.046697	.004193	.047687	.004015

TABLE I (continued)

v	$G_o(v)$	B_o^2
8.2	.042558	.002205
8.4	.039492	.000664
8.6	.038265	.000004
8.8	.039372	.000568
9.0	.042943	.002533
9.2	.048707	.005853
9.4	.056014	.010237
9.6	.063935	.015169
9.8	.071399	.019971
10.0	.077363	.023906

TABLE III

m	$a_{o,m}$	m	$b_{o,m}$	m	$a_{1,m}$	m	$b_{1,m}$
0	+0.00000 -65	1	-4.54747 -13	0	+1.25000 -01	1	-2.08333 -02
1	-4.16666 -02	2	+5.20833 -03	1	-2.60417 -02	2	+8.59374 -03
2	+5.20833 -03	3	-1.43229 -03	2	+1.51909 -03	3	-7.37847 -04
3	-2.17013 -04	4	+9.22309 -05	3	-4.06901 -05	4	+2.59964 -05
4	+4.52112 -06	5	-2.59964 -06	4	+6.21654 -07	5	-4.91672 -07
5	-5.65140 -08	6	+4.09726 -08	5	-6.12235 -09	6	+5.76914 -09
6	+4.70950 -10	7	-4.12081 -10	6	+4.20491 -11	7	-4.59737 -11
7	-2.80327 -12	8	+2.87335 -12	7	-2.12748 -13	8	+2.64684 -13
8	+1.25146 -14	9	-1.47046 -14	8	+8.25617 -16	9	-1.15151 -15
9	-4.34535 -17	10	+5.75760 -17	9	-2.53479 -18	10	+3.91685 -18
10	+1.20704 -19	11	-1.78038 -19	10	+6.30954 -21	11	-1.06985 -20
11	-2.74327 -22	12	+4.45782 -22	11	-1.29890 -23	12	+2.39777 -23
12	+5.19560 -25	13	-9.22219 -25	12	+2.24809 -26	13	-4.48747 -26
13	-8.32629 -28	14	+1.60281 -27	13	-3.31679 -29	14	+7.11966 -29
14	+1.14372 -30	15	-2.37322 -30	14	+4.22087 -32	15	-9.69440 -32
15	-1.36157 -33	16	+3.02949 -33	15	-4.68040 -35	16	+1.14528 -34
16	+1.41830 -36	17	-3.36847 -36	16	+4.56256 -38	17	-1.18496 -37
17	-1.30358 -39	18	+3.29156 -39	17	-3.94058 -41	18	+1.08260 -40
18	+1.06502 -42	19	-2.84893 -42	18	+3.03625 -44	19	-8.79735 -44
19	-7.78526 -46	20	+2.19934 -45	19	-2.09997 -47	20	+6.39979 -47
20	+5.12188 -49	21	-1.52376 -48	20	+1.31095 -50	21	-4.19202 -50
21	-3.04874 -52	22	+9.52731 -52	21	-7.42385 -54	22	+2.48535 -53
22	+1.64975 -55	23	-5.40293 -55	22	+3.83094 -57	23	-1.34001 -56
23	-8.15094 -59	24	+2.79169 -58	23	-1.80885 -60	24	+6.59864 -60

The second number in the column is the number that 10 is raised to to place the decimal.

REFERENCES

(1) R. Mertens, Mendedeling Koninklijke Viaamse Academie Wetenschapen, 12, 1-37 (1950).

(2) R. B. Miller and E. A. Hiedemann, Jour. Acous. Soc. Am., 30, 1042 - 1046, (1958).

Reprinted from THE JOURNAL OF THE ACOUSTICAL SOCIETY OF AMERICA, Vol. 33, No. 12, 1803, December, 1961

Demonstration of the "Least Stable Waveform" of Finite Amplitude Waves

M. A. BREAZEALE AND W. W. LESTER
Department of Physics, Michigan State University, East Lansing, Michigan
(Received July 28, 1961)

A backward-sloping ultrasonic wave is generated by reflection of a finite amplitude distorted wave from a pressure-release boundary. The difference between the behavior of this wave and that of a wave distorted in the usual sense is demonstrated.

As is well known, an ultrasonic wave of large amplitude can undergo distortion so that the slope of its leading edge is much greater than that of its trailing edge. If such a nonsymmetric wave is reflected from a boundary, two extreme cases are possible: The waveform may be unchanged, as in the case of a perfectly rigid reflector, or it may be inverted, as in the case of a perfect pressure-release reflector. For a pressure-release reflector, the resulting waveform would have the slope of its trailing edge greater than the slope of its leading edge. Such a waveform has been described by Fay[1] as the "least stable waveform" in contrast with the more usual case of the most stable waveform. In the least stable waveform the fundamental harmonic component can increase with distance, while the higher harmonics decrease with distance.[2] Thus, an initially distorted wave can become undistorted as it progresses. The following experiment was designed to demonstrate the inversion of waveform on reflection from a pressure-release boundary and this decrease of distortion with distance.

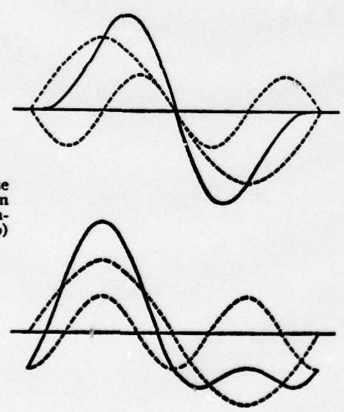

FIG. 1. Effect of phase shift of second harmonic in resonant transducer. (a) Incident distorted wave. (b) resulting CRO wave.

A pressure-release reflector was constructed by stretching a plastic membrane over an air chamber, and a rigid one by mounting an aluminum plate so it could be easily attached in place of the pressure release boundary.

The experiment was performed with high intensity 2-Mc ultrasonic pulses in water. The waveform of the ultrasonic pulse at various distances before and after it had been reflected was monitored by use of a barium titanate transducer. Since the receiver resonated near the second harmonic, this harmonic was accentuated in the waveform displayed on an oscilloscope. Further, the receiver resonance caused a phase shift of almost 90° in the second harmonic component displayed on the oscilloscope. This made it possible to detect very small amounts of second harmonic by observing the "flattening" of the bottom of the oscilloscope trace and the "sharpening" of the top. This is illustrated in Fig. 1. For a distorted wave such as that illustrated in (a) we get the oscilloscope trace shown in (b) when the phase shift of the second harmonic is 90°. The increase of waveform distortion with distance could be observed by watching this type of distortion on the scope. Since there is a phase shift of 180° in each of the harmonics when a rigid reflector is used and 0° when a presssure-release reflector is used, the corresponding oscilloscope traces differed markedly from each other.

Figure 2 gives a series of pictures of oscilloscope traces which show the transducer output at increasing distances from the source. It can be seen that the distortion of the waveform increases with distance. As indicated, reflection from a solid boundary produced the waveforms shown in the second row of pictures where it can be seen that the distortion continues to increase with increasing distance. On the other hand, the lower part of the figure shows that the wave on reflection from a pressure-release boundary is inverted; i.e., it is distorted in the "wrong direction." Therefore, the distortion decreases with increasing distance until at a distance from the pressure-release reflector almost equal to that between the transducer and the boundary, the waveform is again essentially sinusoidal. On progressing farther, the wave becomes sinusoidal and then distorts again. Considerations of this type of distortion might be necessary if one were concerned with reflection of finite amplitude waves from the free surface of liquids.

The authors wish to express their appreciation to Professor E. A. Hiedemann for the interest he has shown in this work, and to the Office of Naval Research for their sponsorship.

[1] R. D. Fay, J. Acoust. Soc. Am. 29, 1200 (1957).
[2] Isadore Rudnick, J. Acoust. Soc. Am. 30, 564 (1958).

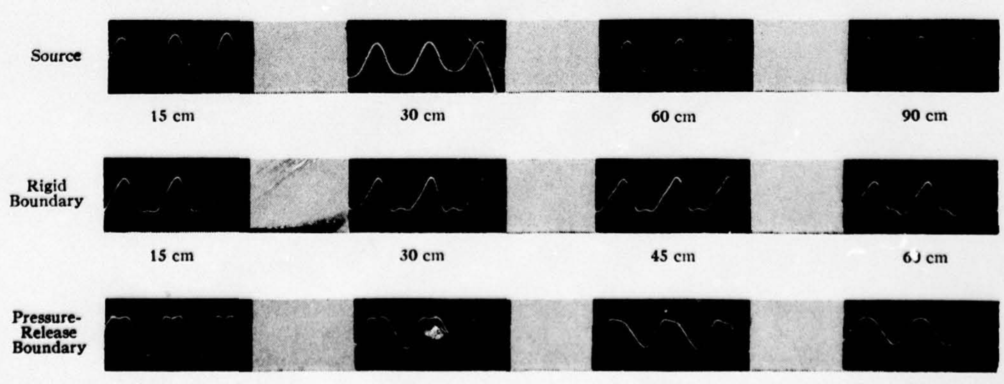

FIG. 2. Distortion of a finite amplitude wave as it progresses from a sinusoidally vibrating source and is reflected from a rigid boundary or a pressure release boundary. The boundaries are 90 cm from the source.

Reprinted from THE JOURNAL OF THE ACOUSTICAL SOCIETY OF AMERICA, Vol. 34, No. 3, 269–270, March, 1962

Optical Method for Ultrasonic Velocity Measurements at Liquid–Solid Boundaries*

WALTER G. MAYER AND JOHN F. KELSEY†
Physics Department, Michigan State University, East Lansing, Michigan
(Received November 24, 1961)

An optical method is used to measure the energy ratio of reflected and incident ultrasonic waves at a liquid-solid interface. The ultrasonic velocities in the solid are calculated from the angles of maximum reflection in the liquid.

THE intensity ratio of reflected to incident ultrasonic waves at a liquid-solid boundary as a function of angle of incidence is given by Ergin[1] as

$$\left(\frac{R}{I}\right)^2=\left[\frac{\cos\beta-A\cos\alpha(1-B)}{\cos\beta+A\cos\alpha(1-B)}\right]^2, \tag{1}$$

where α is the angle of incidence in the liquid measured from a line normal to the interface, β and γ are the angles of refraction of the longitudinal and shear wave in the solid. The quantities A and B are defined by

$$A=\rho_2 V_L/\rho_1 V_I, \tag{2}$$

$$B=2\sin\gamma\sin 2\gamma[\cos\gamma-(V_S/V_L)\cos\beta], \tag{3}$$

where ρ_1 and ρ_2 are the densities of the liquid and the solid, respectively, and V_I is the velocity of the incident wave in the liquid; V_L and V_S are the velocities of the refracted longitudinal and shear waves in the solid.

Substituting accepted values for the densities and velocities of water and Plexiglas in Eq. (1) one obtains the curve shown in Fig. 1(a) for the intensity ratio $(R/I)^2$. Figure 1(b) shows this ratio for a water-aluminum boundary. The ultrasonic wave is incident in the water in both cases. In order to obtain these curves one has to use the appropriate angles β and γ

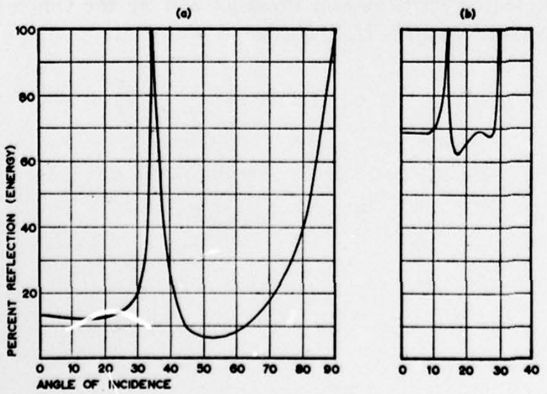

FIG. 1. Intensity ratio of reflected to incident wave as a function of angle of incidence for (a) a water-Plexiglas boundary where $V_S<V_I<V_L$ and (b) a water-aluminum boundary where $V_I<V_S<V_L$.

for a given angle of incidence α. These angles are found from Snell's law

$$V_I/V_L=\sin\alpha/\sin\beta,\quad V_I/V_S=\sin\alpha/\sin\gamma. \tag{4}$$

It can be seen from Eq. (4) that $\sin\alpha=V_I/V_L$ or $\sin\alpha=V_I/V_S$ at the critical angles for the longitudinal and shear wave where $\sin\beta$ or $\sin\gamma$ equal unity. One can obtain V_L and V_S if V_I is known provided the critical angles can be located. Equation (1) and Fig. 1 show that the ratio $(R/I)^2=1$ at the critical angles. The associated peaks in the intensity of the reflected wave can be located experimentally and can be used to calculate V_L and V_S for the solid.[2]

An optical method is used to find the angle of incidence at which the intensities of the reflected and incident beams are equal. The arrangement is shown in Fig. 2. The solid sample and the transducer are

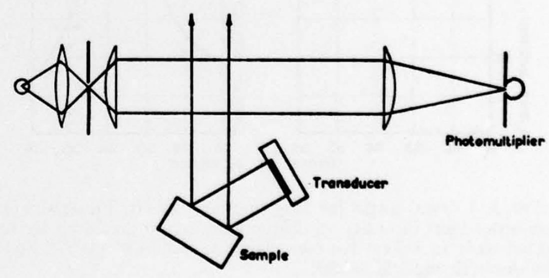

FIG. 2. Diagram of the optical arrangement.

placed in a tank filled with water. While the angle of incidence is changed by rotating the transducer, the sample is also rotated in such a manner that the reflected sound beam remains at right angles to the collimated light beam. The reflected ultrasonic wave produces a diffraction pattern in the plane of the photomultiplier. The light intensity in the nth order of the diffraction pattern is given by

$$I_n=J_n^2(v), \tag{5}$$

where v is proportional to the amplitude of the ultrasonic wave producing the diffraction pattern. Keeping the output of the transducer constant and measuring the light intensity in the zero order, one finds a pronounced dip at that angle of incidence where the reflected ultrasonic wave is most intense. Figure 3(a)

* Presented at the 62nd meeting of the Acoustical Society of America, Cincinnati, November 1961.
† NSF Undergraduate Research Participant.
[1] K. Ergin, Bull. Seism. Soc. Am. 42, 349 (1952).
[2] W. G. Mayer, J. Acoust. Soc. Am. 32, 1213 (1960).

shows the zero order light intensity for an 8-Mc continuous ultrasonic wave reflected from a water-Plexiglas boundary. For convenience the intensity of the incident wave is kept low enough so that the zero-order Bessel function is positive for all possible values of v of the reflected wave. The critical angle is located at 33.5° from which one finds $V_L=2700$ m/sec, using Eq. (4). The velocity in water V_I can be determined by measuring the spacing between the lines of the diffraction pattern produced by the reflected wave in the liquid. Figure 3(b) shows the intensity of the reflected wave obtained from the data given in Fig. 3(a). The theoretical curve predicted by Eq. (1) is also given.

The same technique is used to measure V_S if $V_S>V_I$. In this case the light intensity in the zero order reaches a minimum at the critical angle for the shear wave and remains at that level. An example is given in Fig. 4(a) which shows the measured light intensity in the zero order produced by a wave reflected from a water-glass boundary at angles in the vicinity of the critical angle for the shear wave. The corresponding intensity of the reflected wave is shown in Fig. 4(b). The critical angle for the shear wave is 25.4° corresponding to a shear wave velocity of 3445 m/sec.

It should be noted that this analysis does not include surface waves or plate transmission phenomena. The method given here has the advantage that the velocity of the longitudinal and shear wave in the solid can be calculated without having to observe the waves in the solid directly.

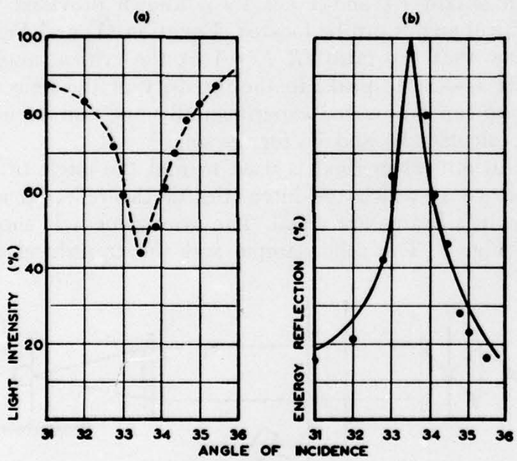

FIG. 3. Critical angle for longitudinal wave in Plexiglas: (a) zero-order light intensity in diffraction pattern produced by reflected wave in water; (b) corresponding values of $(R/I)^2$. Solid line shows theoretical values.

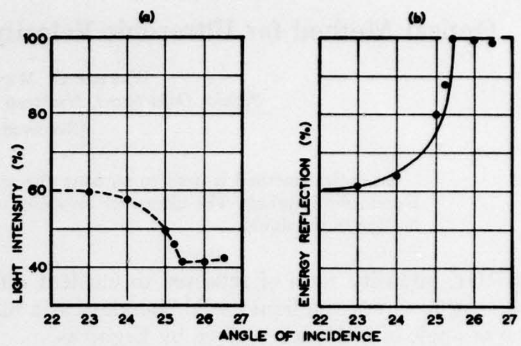

FIG. 4. Critical angle for shear wave in glass: (a) zero-order light intensity in diffraction pattern produced by reflected wave in water; (b) corresponding values of $(R/I)^2$. Solid line shows theoretical values.

ACKNOWLEDGMENTS

The authors wish to thank Professor E. A. Hiedemann for the interest he has shown in this problem.

This work was supported by the NSF Undergraduate Research Participation Program and by the Office of Naval Research, U. S. Navy.

Zeitschrift für Physik 167, 326—336 (1962)

From the Department of Physics, Michigan State University, East Lansing, Michigan and Seminarie voor Wiskundige Natuurkunde, Rijkuniversiteit Gent, Belgium

Diffraction of Light by Two Spatially Separated Parallel Ultrasonic Waves of Different Frequency*

By

L. E. HARGROVE, E. A. HIEDEMANN and ROBERT MERTENS**

With 5 Figures in the Text

(Received January 8, 1962)

* This work was supported in part by the U.S. Army Research Office (Durham) and the Office of Naval Research, U. S. Navy.

** Geassocieerde van het National Fonds voor Wetenschappelijk Onderzoek van België.

A theory is developed for the diffraction of light by two spatially separated parallel ultrasonic progressive waves of different frequency. The preliminary theories of RAMAN and NATH [C. V. RAMAN and N. S. NATH, Proc. Indian Acad. Sci. A **2**, 406–412; 413–420 (1935)] for normal and oblique incidence are taken to be valid. The resulting equations are extensions of earlier results of R. MERTENS, Z. Physik **160**, 291–296 (1960). The predicted periodicity of the diffraction spectrum with increasing sound beam separation agrees with the well known periodicity of the light intensity distributions in the Fresnel zone of the phase grating formed by the first ultrasonic wave. Results of numerical calculations are presented to illustrate features of the theoretical results, as reflected in the first order of diffraction for 3·0 and 6·0 Mc ultrasonic waves in water.

Introduction

Theoretical results have been given by RAO[1], MURTY[2], and MERTENS[3] for diffraction of a wide light beam by an ultrasonic wave consisting of two commensurable frequency components with arbitrary relative phase. These theoretical results are for *simultaneous* diffraction of light by the two frequency components contained in the *same* sound beam. MERTENS[4] recently pointed out that simultaneous diffraction and *successive* diffraction by two separate parallel ultrasonic beams are not the same. MURTY and RAO[5] obtained very good agreement between their experimental results from a successive diffraction experiment and

[1] RAO, B. R.: Proc. Indian Acad. Sci. A **29**, 16–27 (1949).
[2] MURTY, J. S.: J. Acoust. Soc. Amer. **26**, 970–974 (1954).
[3] MERTENS, R.: Proc. Indian Acad. Sci. A **8**, 288–306 (1958).
[4] MERTENS, R.: Z. Physik **160**, 291–296 (1960).
[5] MURTY, J. S., and B. R. RAO: Z. Physik **157**, 189–197 (1959). The agreement obtained is indeed surprising, as it is doubtful that *progressive* waves were obtained at 3.0 and 1.5 Mc in a metal tank only 12 in. long.

values calculated from simultaneous diffraction theory. Also, the diffraction effects of two parallel ultrasonic waves have proven useful, in a limited range, in investigations[6,7] of finite-amplitude distortion: Simultaneous diffraction theory was used. But, as MERTENS has stated, simultaneous and successive diffraction differ negligibly for the cases considered experimentally by MURTY and RAO. In a limited range, simultaneous and successive diffraction spectra are indistinguishable. HARGROVE[8] made some preliminary experimental studies of successive diffraction and reported qualitative, but lack of quantitative, agreement between his experimental results and simultaneous diffraction theory. MERTENS'[4] paper, giving expressions for the amplitudes of light diffracted by two parallel, adjacent (no space between), ultrasonic beams with integer frequency ratio and arbitrary relative phase, appeared shortly after the experimental results of HARGROVE were reported. The present theoretical development was undertaken to include the spatial separation of ultrasonic beams which existed in the experimental arrangement of HARGROVE.

RAMAN and NATH[9,10] developed a theory to explain the diffraction of light by sound for the case of a wide plane wave of light passing through a plane sinusoidal ultrasonic wave at normal incidence. The theory predicts that the light is diffracted at discrete angles given by

$$\sin \vartheta_r = - r\lambda/\lambda^*, \tag{1}$$

where r is zero or a positive or negative integer, and λ and λ^* are the wavelengths of light and sound, respectively. Equation (1) is valid for any plane periodic sound wave. The Raman-Nath theory predicts that for a progressive sinusoidal ultrasonic wave the normalized intensity I_r in the r-th order of diffraction is

$$I_r = J_r^2(v), \tag{2}$$

where the Raman-Nath parameter v is approximately proportional to the sound pressure amplitude and given by

$$v = 2\pi\mu L/\lambda, \tag{3}$$

where μ is the peak change in refractive index caused by the sound pressure and L is the width of the sound beam. Equation (2) is valid if the light wavefront can be considered to be changed only in relative phase as it passes through the sound beam. This assumption has been

[6] ZANKEL, K. L.: J. Acoust. Soc. Amer. 32, 707–713 (1960).
[7] MAYER, W. G., and E. A. HIEDEMANN: J. Acoust. Soc. Amer. 32, 706–708 (1960).
[8] HARGROVE, L. E.: J. Acoust. Soc. Amer. 32, 940 (A) (1960).
[9] RAMAN, C. V., and N. S. NATH: Proc. Indian Acad. Sci. A 2, 406–412 (1935).
[10] RAMAN, C. V., and N. S. NATH: Proc. Indian Acad. Sci. A 3, 75–84 (1936).

considered justifiable[11,12] for conditions under which

$$(2\pi L \lambda v)/(\mu_0 \lambda^{*2}) \leqq N, \tag{4}$$

where μ_0 is the refractive index of the undisturbed medium and N lies in a range $1 \leqq N \leqq 2$, depending on the accuracy required.

Proceeding from assumed validity of the Raman-Nath theory, we shall obtain expressions for the diffraction of light by two spatially separated parallel ultrasonic waves of different frequency. This development follows the method used by MERTENS[4] and extends his results to more general cases. Some results of numerical calculations will be presented to illustrate the dependence of the first diffraction order light intensity on various parameters.

Development of the Theory

Consider two parallel ultrasonic beams with width L_m and L_n separated by a distance L' as indicated in Fig. 1. Let plane monochromatic

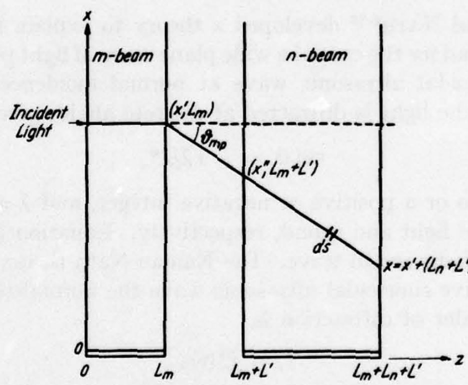

Fig. 1. Coordinate axis for the case of two spatially separated parallel ultrasonic beams and the schematic path of a typical light ray

light be incident in the $+z$-direction. The first sound beam produces a change in refractive index given by

$$\mu_m(x,t) = \mu_0 + \mu_m \sin 2\pi\,(m\,v^* t - m\,x/\lambda^* + \delta_m/2\pi) \tag{5}$$

where v^* is the ultrasonic fundamental frequency and δ_m is the relative phase of the m-th harmonic. Similarly, for the second sound beam,

$$\mu_n(x,t) = \mu_0 + \mu_n \sin 2\pi\,(n\,v^* t - n\,x/\lambda^* + \delta_n/2\pi). \tag{6}$$

[11] EXTERMANN, R., and G. WANNIER: Helv. phys. Acta 9, 520–532 (1936).
[12] RYTOV, S. M.: Diffraction de la lumière par les ultra-sons. Actualités scientifiques et industrielles, 613. Paris: Hermann & Cie. 1938.

We have assumed that there exists a fundamental frequency ν^* such that n and m are integers. The enumeration of diffraction orders and the corresponding diffraction angles shall be those pertaining to the fundamental frequency.

According to the preliminary theory of RAMAN and NATH, the light amplitude at the point (x', L_m) is given by

$$\left.\begin{aligned}\varphi(x', L_m) &= \exp\left[\frac{-2\pi i L_m \mu_0}{\lambda}\right] \times \\ &\times \exp\left[-i v_m \sin 2\pi(m\nu^* t - m x'/\lambda^* + \delta_m/2\pi\right] \exp(2\pi i \nu t),\end{aligned}\right\} \quad (7)$$

where ν is the frequency of the incident light. From the identity

$$\exp(-ia\sin b) = \exp[ia\sin(-b)] = \sum_{p=-\infty}^{+\infty} J_p(a)\exp(-ipb), \quad (8)$$

Eq. (7) becomes

$$\left.\begin{aligned}\varphi(x', L_m) &= \exp\left[\frac{-2\pi i L_m \mu_0}{\lambda}\right] \exp(2\pi i \nu t) \sum_{p=-\infty}^{+\infty} J_p(v_m) \times \\ &\times \exp\left[2\pi i p\,(m x'/\lambda^* - m\nu^* t - \delta_m/2\pi)\right].\end{aligned}\right\} \quad (9)$$

Consider now the p-th term of Eq. (9) which represents light propagating in the direction $\vartheta_{mp} = -\sin^{-1}[m p \lambda/\mu_0 \lambda^*]$ with amplitude $J_p(v_m)$. This light component progresses to the plane $z = L_m + L'$ through medium undisturbed by ultrasonic waves. However, the light path (see Fig. 1) is displaced from x' to x''. At the point $(x'', L_m + L')$ the amplitude of the p-th component is

$$\left.\begin{aligned}\varphi_p(x'', L_m + L') &= \exp\left[\frac{-2\pi L' \mu_0}{\lambda\cos\vartheta_{mp}}\right] \exp\left[\frac{-2\pi i L_m \mu_0}{\lambda}\right] \times \\ &\times \exp\left[2\pi i(\nu - m p \nu^*)\,t\right] \exp\left[\frac{2\pi i p m x'}{\lambda^*}\right] \exp(-ip\,\delta_m)\,J_p(v_m).\end{aligned}\right\} \quad (10)$$

Equation (10) expresses the amplitude of the plane wave of light incident on the second sound beam, making an angle ϑ_{mp} with the z-axis. Using the Raman-Nath elementary theory for oblique incidence[13], Eq. (10) must be multiplied by

$$\exp\left[(-2\pi i/\lambda) \int_0^{L_n/\cos\vartheta_{mp}} \mu_n(s, t)\,ds\right], \quad (11)$$

where the integral in (11) represents the optical path length of the p-th component in the second sound beam. The coefficient of this integral should be $-2\pi i(\nu - m p \nu^*)/c$ but is here approximated by $-2\pi i/\lambda$

[13] RAMAN, C. V., and N. S. NATH: Proc. Indian Acad. Sci. A **2**, 413–420 (1935).

since $\nu^* \ll \nu$ and only a few terms of Eq. (9) are significant. From Eq. (2) we obtain

$$\mu_n(s, t) = \mu_0 + \mu_n \sin 2\pi [n \nu^* t - n(x - s \sin \vartheta_{mp})/\lambda^* + \delta_n/2\pi]. \quad (12)$$

The intregal in (11) then becomes

$$\left.\begin{aligned} \int_0^{L_n/\cos\vartheta_{mp}} \mu_n(s, t)\, ds = \frac{\mu_0 L_n}{\cos\vartheta_{mp}} + \frac{\mu_n \lambda^*}{n\pi \sin\vartheta_{mp}} \times \\ \times \sin\left[2\pi n\left(\nu^* t - \frac{x}{\lambda^*} + \frac{L_n}{2\lambda^*}\tan\vartheta_{mp}\right) + \delta_n\right] \sin\left[\frac{n\pi L_n}{\lambda^*}\tan\vartheta_{mp}\right]. \end{aligned}\right\} \quad (13)$$

The value of the integral is substituted into (11) and this result multiplies Eq. (10). The result of this multiplication is expanded (q = summation index) according to Eq. (8). The q-th component represents the amplitude of a final light component which has been successively diffracted ϑ_{mp} by the first sound beam and ϑ_{nq} by the second sound beam, and is given by

$$\left.\begin{aligned} \varphi_{pq} = J_p(v_m)\, J_q\left\{\frac{v_n \lambda^*}{n\pi L_n \sin\vartheta_{mp}} \sin\left[\frac{n\pi L_n}{\lambda^*}\tan\vartheta_{mp}\right]\right\} \times \\ \times \exp[-i(p\,\delta_m + q\,\delta_n)] \exp\left[\frac{-2\pi i m p}{\lambda^*}(L_n + L')\tan\vartheta_{mp}\right] \times \\ \times \exp\left[\frac{-2\pi i n q}{\lambda^*}(L_n/2)\tan\vartheta_{mp}\right] \exp\left[\frac{-2\pi i \mu_0}{\lambda}\,\frac{(L_n + L')}{\cos\vartheta_{mp}}\right]. \end{aligned}\right\} \quad (14)$$

Time and space terms which do not contribute to the final intensities have been deleted from Eq. (14). In the argument of the last exponential factor (with $L' = 0$), MERTENS[4] essentially approximated $1/\cos\vartheta_{mp}$ by unity and this term no longer contributed to the final intensities. However, as this last exponential factor accounts for the *different* optical phases of the light components which combine to form a given order of the final spectrum, we must retain it. The different phases arise from the different (for different p) path lengths from the plane $z = L_m$ to the plane $z = L_m + L_n + L'$ in a medium with refractive index μ_0. The next to last exponential factor in Eq. (14) expresses the effect of the average ultrasonic phase difference (i.e., in addition to δ_m and δ_n) along the oblique light path through the second sound beam. The second exponential factor expresses the effect of the additional ultrasonic phase difference between the points (x', L_m) and $(x, L_m + L_n + L')$ of emergence of light from the two ultrasonic beams. The effect of the actual phase differences of the two ultrasonic waves is expressed by the first exponential factor in a manner identical with that for simultaneous diffraction. The factors multiplying v_n in the argument of the Bessel function of order q give an effective Raman-Nath parameter for oblique incidence.

The r-th order of the final spectrum with frequency $(\nu - r\,\nu^*)$ makes an angle $\vartheta_r = \vartheta_{mp} + \vartheta_{nq}$ with the z-axis. Summing all φ_{pq} such that

$mp + nq = r$ we obtain the amplitude in the r-th order to be

$$\varphi_r = \sum_{p,q=-\infty}^{+\infty}{}' \varphi_{pq} \tag{15}$$

where the prime on the summation indicates summation on all integer values of p and q such that $mp + nq = r$, $r = 0$ or positive or negative integers.

For the special cases $m = 1$ and $\delta_m = 0$ or $n = 1$ and $\delta_n = 0$, the summations can be written in a straightforward manner with a single summation index and no prime on the sum.

For $m = 1$, $p = r - nq$ (always an integer) giving

$$\left.\begin{aligned}\varphi_r = \sum_{q=-\infty}^{+\infty} J_{r-nq}(v_1)\, J_q \left\{\frac{v_n \lambda^*}{n \pi L_n \sin \vartheta_{r-nq}} \sin\left[\frac{n \pi L_n}{\lambda^*} \tan \vartheta_{r-nq}\right]\right\} \times \\ \times \exp(-iq\delta_n) \exp\left[\frac{-2\pi i (r-nq)}{\lambda^*}(L_n + L') \tan \vartheta_{r-nq}\right] \times \\ \times \exp\left[\frac{-2\pi i nq}{\lambda^*}(L_n/2) \tan \vartheta_{r-nq}\right] \exp\left[\frac{-2\pi i \mu_0}{\lambda} \frac{(L_n + L')}{\cos \vartheta_{r-nq}}\right].\end{aligned}\right\} \tag{15'}$$

For $n = 1$, $q = r - mp$ (always an integer) giving

$$\left.\begin{aligned}\varphi_r = \sum_{p=-\infty}^{+\infty} J_p(v_m)\, J_{r-mp} \left\{\frac{v_1 \lambda^*}{\pi L_n \sin \vartheta_{mp}} \sin\left[\frac{\pi L_n}{\lambda^*} \tan \vartheta_{mp}\right]\right\} \times \\ \times \exp(-ip\delta_m) \exp\left[\frac{-2\pi i mp}{\lambda^*}(L_n + L') \tan \vartheta_{mp}\right] \times \\ \times \exp\left[\frac{-2\pi i (r-mp)}{\lambda^*}(L_n/2) \tan \vartheta_{mp}\right] \times \\ \times \exp\left[\frac{-2\pi i \mu_0}{\lambda} \frac{(L_n + L')}{\cos \vartheta_{mp}}\right].\end{aligned}\right\} \tag{15''}$$

Equations (15′) and (15″) with $L' = 0$ correspond to MERTENS[4] Eqs. (9) and (11) respectively.

We may express φ_r in approximate forms which are more suitable for numerical calculations by using

$$\vartheta_k \approx \tan \vartheta_k \approx \sin \vartheta_k = -k\lambda/(\mu_0 \lambda^*), \tag{16}$$

$$1/\cos \vartheta_k = \sec \vartheta_k \approx 1 + \vartheta_k^2/2, \tag{17}$$

and the variables

$$Q = \frac{2\pi\lambda}{\mu_0 \lambda^{*2}} L_n \quad \text{and} \quad Q' = \frac{2\pi\lambda}{\mu_0 \lambda^{*2}} L'. \tag{18}$$

Use of (16), (17), and (18) gives the approximate form of Eq. (15) to be

$$\left.\begin{aligned}\varphi_r = \sum_{p,q=-\infty}^{+\infty}{}' J_p(v_m)\, J_q\left[v_n \frac{\sin \frac{1}{2} nmpQ}{\frac{1}{2} nmpQ}\right] \exp[-i(p\delta_m + q\delta_n)] \times \\ \times \exp\left[\frac{1}{2} imp nqQ + \frac{1}{2} im^2 p^2 (Q + Q')\right].\end{aligned}\right\} \tag{19}$$

For $m=1$ the approximate form is

$$\left.\begin{aligned}\varphi_r = \sum_{q=-\infty}^{+\infty} J_{r-nq}(v_1)\, J_q\left[v_n \frac{\sin \frac{1}{2} n\,(r-nq)\,Q}{\frac{1}{2} n\,(r-nq)}\right] \exp(-i q\,\delta_n) \times \\ \times \exp\left[\frac{1}{2}\, i\, n q\,(r-nq)\,Q + \frac{1}{2}\, i\,(r-nq)^2 (Q+Q')\right].\end{aligned}\right\} \tag{19'}$$

For $n=1$ the approximate form is

$$\left.\begin{aligned}\varphi_r = \sum_{p=-\infty}^{+\infty} J_p(v_m)\, J_{r-mp}\left[v_1 \frac{\sin \frac{1}{2} m p\,Q}{\frac{1}{2} m p\,Q}\right] \exp(-i p\,\delta_m) \times \\ \times \exp\left[\frac{1}{2}\, i\, m\, p\,(r-mp)\,Q + \frac{1}{2}\, i m^2 p^2 (Q+Q')\right].\end{aligned}\right\} \tag{19''}$$

The more useful results are summarized in these last three equations. The light intensities are obtained from

$$I_r = |\varphi_r|^2. \tag{20}$$

Discussion

The inclusion of the space L' between the two sound beams is a newly added parameter in the theory of successive diffraction. In most experimental arrangements there will be some beam separation necessary to accomodate the crystal mountings. Let us first consider the effect on diffraction of the beam separation L'. From Eq. (19) we see that the dependence of light amplitude on L' is expressed by the factor

$$\exp\left(\tfrac{1}{2}\, i m^2 p^2 Q'\right) \tag{21}$$

and, being independent of n and q, (21) depends only on L' and parameters pertaining to the first ultrasonic beam. The character of the diffraction spectrum should be periodic as the argument of (21) changes by integral multiples of 2π for all values of p. By expressing the argument of (21) in terms of L', taking $p=1$, and equating the result to $2P\pi$, where P is a positive integer, we obtain the periodicity relationship

$$L'_P = 2P\,(\mu_0\, \lambda^{*2}/m^2\, \lambda). \tag{22}$$

Using $\lambda^*_m = \lambda^*/m$ we now note that

$$L'_P = 2P\,(\mu_0\, \lambda^{*2}_m/\lambda) = 2PD \tag{23}$$

where D is the distance from $z=L_m$ in which the phase modulated wavefront at $z=L_m$ reappears, as predicted by NATH[14] for progressive waves. At $z=L_m+D$ the light wavefront is the same as at $z=L_m$ except for being shifted by $\lambda^*_m/2$ in the x-direction. Thus we see that the effect

[14] NATH, N. S.: Proc. Indian Acad. Sci. A 4, 262–274 (1936).

of L' equal to *odd* multiples of D is the same as changing λ_m by $\pm\pi$ radians with $L'=0$. Furthermore, the diffraction spectra for any L' plus integral multiples of $2D$ are identical. These periodicity features will be illustrated with numerical examples.

Numerical calculations of the positive first-order light intensities were made using an electronic computer. Several of the parameters were chosen identical with those for which one of the authors has experimentally investigated simultaneous[15] and successive[8] diffraction. The fixed parameters used for calculations are $\nu^* = 3{\cdot}0$ Mc, $\lambda^* = 0{\cdot}5$ mm

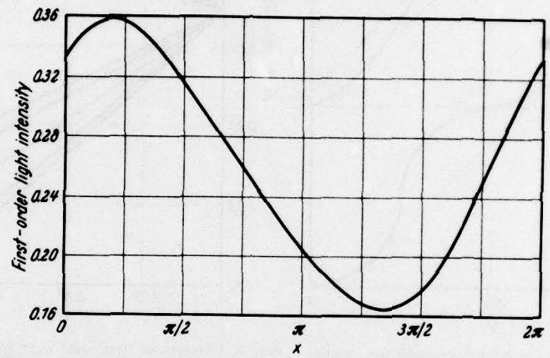

Fig. 2. First-order light intensity *vs* the variable X; $a_2 = 0{\cdot}200$ and $Q' = 5\pi/16$

(water), $\lambda = 5461$ A, $m=2$, $n=1$, $\mu_0 = 1{\cdot}33$ (water), $L_m = L_n = 2{\cdot}0$ cm and $v_1 = 2{\cdot}40$. The equation used for calculation, obtained from Eq. (15″), was

$$I_{+1} \approx \left| \sum_{p=-2}^{+2} J_p(v_2)\, J_{1-2p}\left[\frac{v_1 \sin pQ}{pQ}\right] \exp\left[2\,i p^2 Q' + i p\,(Q-\delta_2)\right] \right|^2 . \tag{24}$$

Equation (24) was evaluated for $a_2 = v_2/v_1$ from 0 to $0{\cdot}200$ in intervals of $0{\cdot}025$, $X = (Q - \delta_2)$ from 0 to 2π in intervals of $\pi/16$, and Q' from 0 to π in intervals of $\pi/16$. For $a_2 = 0{\cdot}200$ calculations were also made for Q' from 0 to $\pi/4$ in intervals $\pi/64$.

As one varies the relative phase between the two sound beams, the intensities in the diffraction orders oscillate. Our attention shall be limited to amplitude and phase of the oscillations of the first-order light intensity and the effect on them of the ratio a_2 and the sound beam separation as expressed by the variable Q'.

Typical first-order light intensity *vs* the variable X is shown in Fig. 2. Note that the extrema of the intensity in this case do not occur for X

[15] Hargrove, L. E., and E. A. Hiedemann: J. Acoust. Soc. Amer. **33**, 1747–1749 (1961).

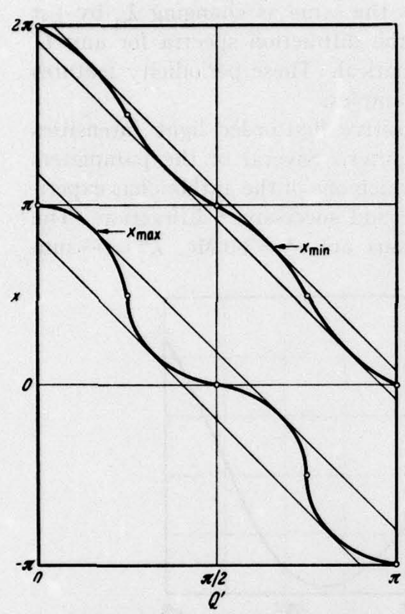

Fig. 3. The values of X corresponding to extreme values of first-order light intensity *vs* Q', for $a_2 = 0{\cdot}200$. The open circles indicate exact values at Q' equal to integral multiples of $\pi/4$, independent of a_2

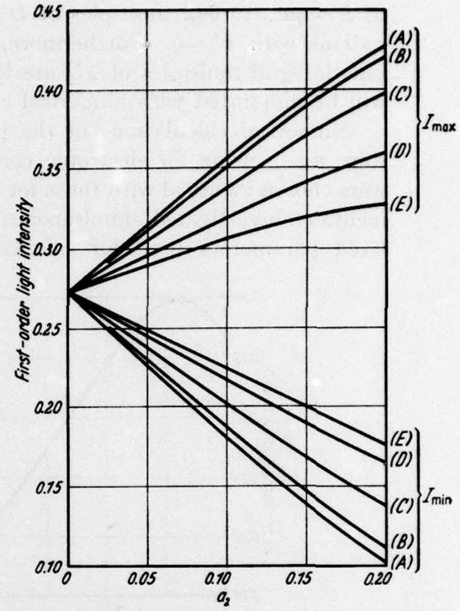

Fig. 5. Extrema of first-order light intensity *vs* the ratio a_2 for various values of Q': (A) $Q' = k\pi/2$, (B) $Q' = k\pi/2 \pm \pi/16$, (C) $Q' = k\pi/2 \pm \pi/8$, (D) $Q' = k\pi/2 \pm 3\pi/16$, (E) $Q' = k\pi/2 \pm \pi/4$, where k is zero or integral such that $Q' \geqq 0$

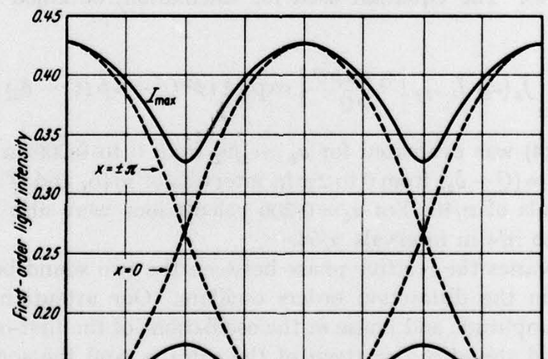

Fig. 4. Extrema of first-order light intensity with respect to variation in relative phase and first-order light intensity for fixed relative phase, *vs* Q', $a_2 = 0{\cdot}200$.

(nor for δ_2) equal to integral multiples of π, and that the curve is not symmetric about the extrema. For the case of simultaneous diffraction, the relative phases for extrema are integral multiples of π. For the case of successive diffraction, the relative phases for extrema depend on both Q and Q' and also, in general, on the amplitudes of the separate sound beams. For the special cases Q' equal to integral multiples of $\pi/4$, the phases for extrema appear to be independent of a_2. Figure 3 shows the values of X corresponding to extrema of the first-order light intensity, with respect to variation of X, *vs* Q' for $a_2 = 0{\cdot}200$. The curves for X_{Max} and X_{Min} for Q' not equal to integral multiples of $\pi/4$ are approximate because the location of extrema was estimated from calculations made in discrete intervals of the appropriate variable. Symmetry of numerical values about the extreme values for Q' equal to integral multiples of $\pi/4$ indicated that these calculated values are truly extrema and that the intensity *vs* X curves are symmetric about the extrema for these special values of Q'.

Figure 4 shows the extrema of first-order light intensity with respect to variation of relative phase, for $a_2 = 0{\cdot}200$, *vs* Q'. This clearly illustrates the periodicity of the diffraction with beam separation. Another illustration of the periodicity is also shown in Fig. 4. The first-order light intensity for constant X and $a_2 = 0{\cdot}200$ *vs* Q' is shown for $X = 0$ and for $X = \pm\pi$ (i.e., for $\delta_2 = Q$ and $\delta_2 = Q \pm \pi$). Note, in Fig. 4, the difference between extrema (with the corresponding changes in relative phase) and the intensity variation with fixed relative phase. The particular fixed relative phases $X = 0$ and $X = \pm\pi$ are chosen here for comparison because these give extrema for $Q' = 0, \pi/2, \pi, \ldots$.

The effect of the ratio a_2 on the extrema of first-order light intensity is shown in Fig. 5. The extrema are shown as a function of a_2 for various values of Q'. Calculations[15] of the extrema from *simultaneous* diffraction theory differ from those for $Q' = 0$ by at most the order of 10^{-3} of the total unit light intensity. However, the differences in predicted extrema for larger Q' are shown here to be significant.

We should remark that the more interesting applications of successive diffraction theory are to those cases for which the results differ significantly from the case of simultaneous diffraction. The simultaneous diffraction equation equivalent to Eq. (19) is

$$\varphi_r = \sum_{p,q}{}' J_p(v_m)\, J_q(v_n) \exp\left[-i\,(p\,\delta_m + q\,\delta_n)\right]. \tag{25}$$

Equation (19) reduces to Eq. (25) as Q and Q' approach zero. For sufficiently small values of $\frac{1}{2}\,n\,m\,p\,Q$ the argument of the Bessel function of order q in Eq. (19) is negligibly different from v_n. Furthermore, for approximate equivalence between successive and simultaneous diffraction, the argument of the last exponential factor in Eq. (19) must be small for all values of p giving significant contributions to the sum. We conclude that the difference between successive and simultaneous diffraction is most marked for Q and/or Q' large. But we must recall that complete validity of the preliminary Raman-Nath theories for normal and oblique incidence has been assumed in the development of the successive diffraction theory. The limitation on the Raman-Nath results formulated in Eq. (4) is closely related to the parameter Q by the relationship

$$Q \leqq N/v \tag{26}$$

for the *fundamental* frequency. This indicates that the product $Q v n^2$ must be less than a number in the range 1 to 2, *depending on the accuracy required*. An analogous limitation applies to the first sound beam. In the case of successive diffraction, where the final diffraction spectrum depends greatly on the amplitude *and* phase of the various light components emerging from the first sound beam, the limitation expressed by

$$(2\pi L_m \lambda v_m)/(\mu_0 \lambda_m^{*2}) \leqq N, \qquad 1 \leqq N \leqq 2, \tag{27}$$

may not be sufficiently stringent. It remains to be shown that there exists a range of the various parameters for which (1) the Raman-Nath theories are sufficiently accurate and (2) the difference between successive and simultaneous diffraction is significant. Reasonable experimental agreement might be obtained for Q small and arbitrary Q', since Q' does not affect validity of the Raman-Nath theories but can give significant difference between successive and simultaneous diffraction.

Pressure Variation of the Index of Refraction of Liquids.

by

M. A. Breazeale

Introduction.

Results of the study of the propagation of light in liquids under pressure can be used directly in the study of the diffraction of light by ultrasonic waves. This fact, though it is sufficient justification for the study, is only one aspect of the overall problem, since it might also be possible to gain basic information about the structure of the liquid if this phenomenon were completely understood.

It has been pointed out repeatedly that the equation given by Lorenz[1] and Lorentz[2], while it is well founded theoretically, is not as accurate in relating the index of refraction and density of a liquid as, for example, the Eykman[3] formula, which is a completely empirical relation. Willard[4] has proposed using the Eykman formula to calculate the change of index of refraction with pressure in the study of ultrasonic waves in water by optical methods. Although Willard did not completely justify the use of this formula, since he referred to the work of Gibson and Kincaid who worked only with benzene, it will be seen that the data collected here will support its use with water, carbon tetrachloride, benzene, and methyl alcohol. These data are collected to show how the values obtained by use of the three relationships agree with those obtained by various experimenters, and hence to give a most probable value of $1/\beta \, dn/dp$ to be used in such experiments as the measurement of ultrasonic pressure amplitude using optical methods. Further, it is suggested that the Gladstone-Dale relation be used since it combines the advantage of simplicity with accuracy.

Discussion of Data

These data are taken primarily from the papers by Raman and Venkataraman[5] by Gibson and Kincaid[6], and Waxler[7] of the Bureau of Standards who used the Gibson and Kincaid pressure vessel and a Pulfrich refractometer for making measurements.

In evaluating dn/dp, cognizance was taken of the fact that the curve relating n and p is not linear, and thus, dn/dp is a function of p, in general decreasing with increasing p. Since the ultrasonic measurements are made at relatively low pressures, of the order of one atmosphere, an attempt was made to evaluate the slope dn/dp at p = 0. This was an approximate procedure because of the way the data was taken. The data was taken at fairly large pressure intervals. Thus, it would be expected that the values given would tend to be smaller than the ones for p = 0 because of the curvature of the pressure-index of refraction relationship. The typical curvature of this relationship is shown in figure 1, which is a plot of some of the data of Gibson and Kincaid. From this curve can be seen the accuracy of the determination of the slope at p = 0. For example, because of the large separation of the experimental points, the slope drawn on the 25° curve could be 10 percent lower if it actually passed through the second experimental point. One might estimate that the accuracy of the slope is something $\pm$ 10 percent. The data for water shown in Figure 2 from Waxler is more linear. Hence, the estimation of the slope is more accurate. It would be still better if the experimental points had been taken at lower pressures. This is the reason for the fact that Raman and Venkatareman used an interferometric method for making measurements. Because of the extreme sensitivity of this method, they were able to make measurements when the pressure changes were of the order of 10 centimeters of mercury. They measured both isothermal and adiabatic values. Naturally, the adiabatic values are of more interest if one is studying the propagation of ultrasonic waves using light diffraction. It is to be noted, however, that in general the difference between the adiabatic and the isothermal values is less than the difference expected because of experimental inaccuracy in the ultrasonic experiments. For example, the difference between the adiabatic and the isothermal values of dn/dp for water as measured by Raman and Venkataraman is 0.2 percent. For carbon disulphide it is 2 percent, which is the largest difference for any liquid given by them. In most cases, therefore, isothermal values will be sufficiently accurate for ultrasonic experiments.

Table 1 is a compilation of the available values of the piezo-optic coefficient. Only Raman and Venkataraman give adiabatic values. For comparison, values are given for both the Lorenz-Lorentz equation and the

Eykman formula. As has been pointed out by Raman and Venkataraman, the Lorenz-Lorentz equation gives values for $1/\beta\ (dn/dp)$ which are too large. Without exception, the Eykman formula gives lower values, and almost without exception, this lower value agrees better with the experimental ones. On the other hand, the Gladstone-Dale relation gives values which are usually lower than the experimental ones and which agree almost as well as those given by the Eykman formulas. Therefore, it might be concluded that in the absence of experimental data the Gladstone-Dale relation is to be preferred.

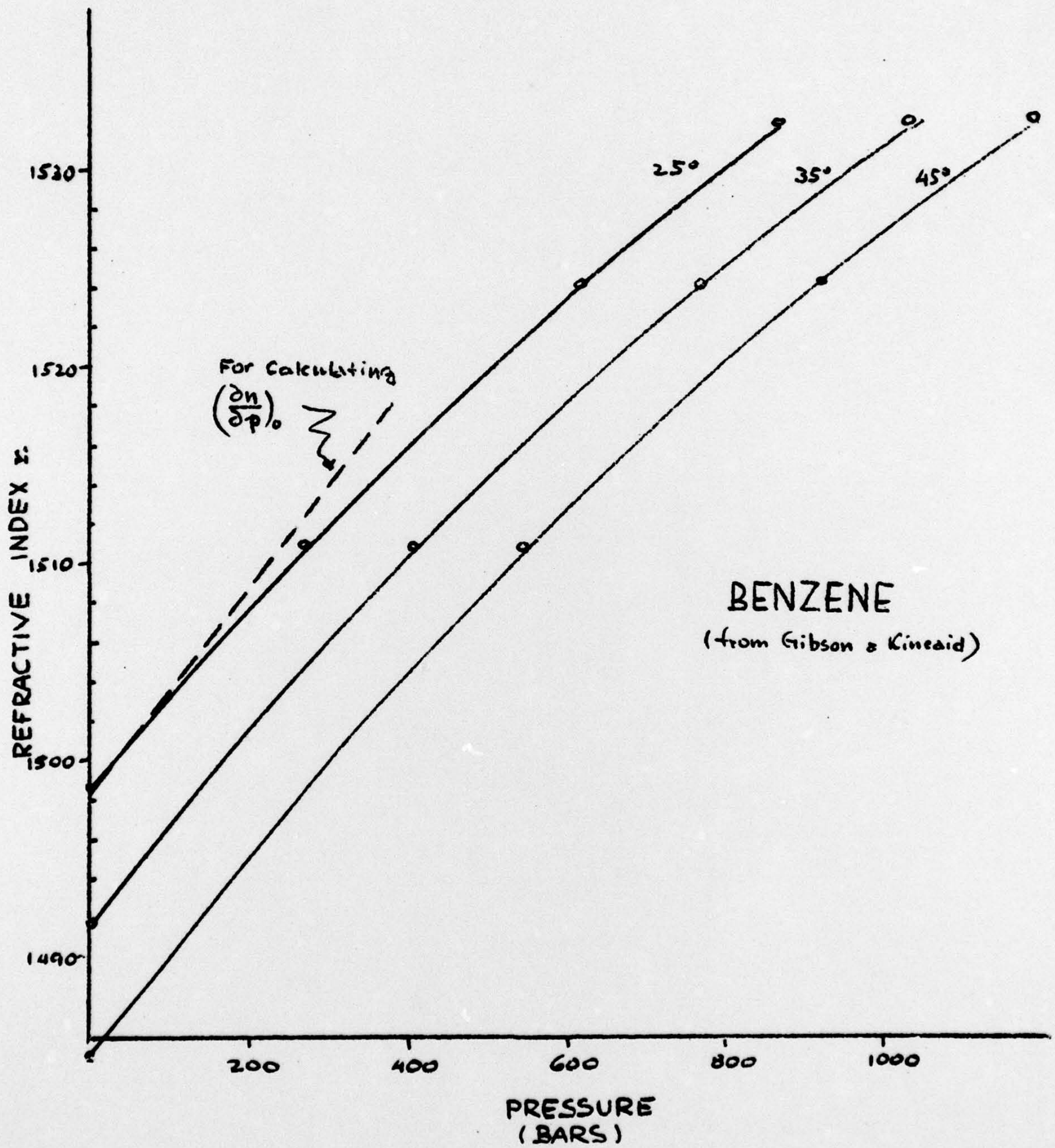

REFRACTIVE INDEX x:
1530
1520
1510
1500
1490
200
400
600
800
1000
PRESSURE
(BARS)
25°
35°
45°
For Calculating
$\left(\frac{\partial n}{\partial p}\right)_0$
BENZENE
(from Gibson & Kincaid)

FIGURE 1

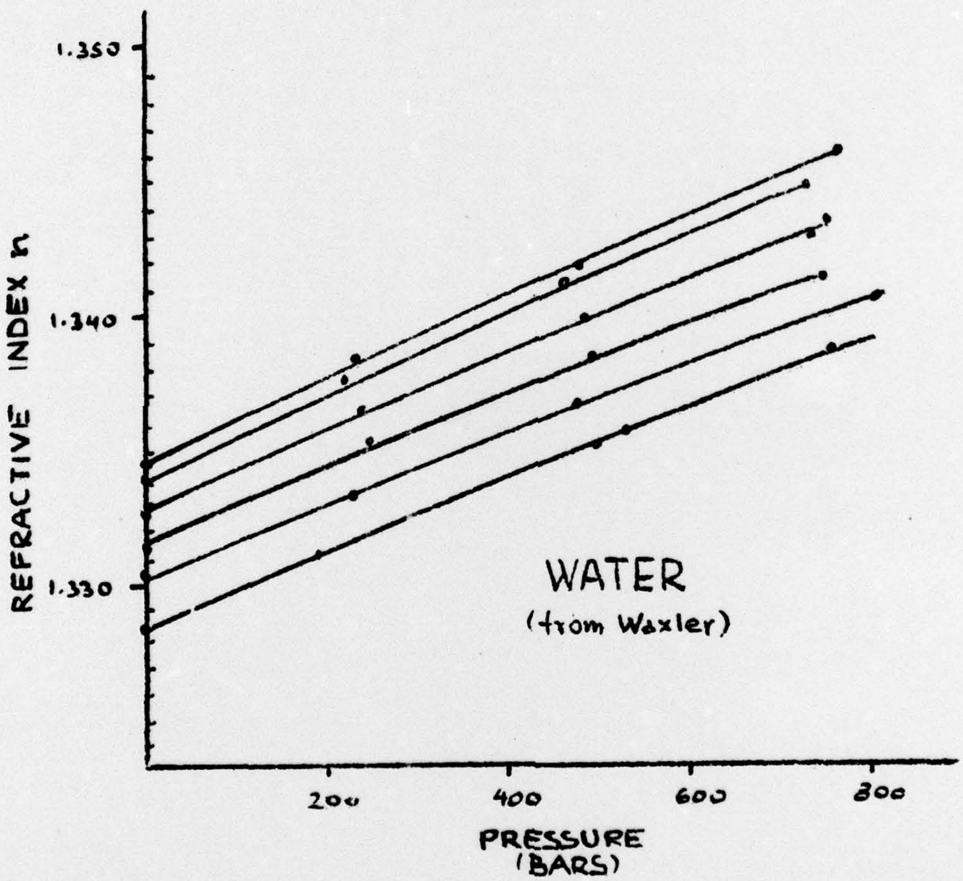
1.350
1.340
1.330
REFRACTIVE INDEX n
WATER
(from Waxler)
200
400
600
800
PRESSURE
(BARS)

FIGURE 2

Table 1.

$$v \frac{dn}{dv} = \frac{1}{\beta T}\left(\frac{\partial n}{\partial p}\right)_T$$

	T	n	Waxler	Lorenz Lorentz	Eykman	Gladstone-Dale	Raman and Venkataraman		Gibson and Kincaid
			$\frac{1}{\beta}\left(\frac{\partial n}{\partial p}\right)_T$	$\frac{(n^2-1)(n^2+2)}{6n}$	$\frac{(n^2-1)(n+0.4)}{n^2+0.8n+1}$	$(n-1)$	$\frac{1}{\beta}\left(\frac{\partial n}{\partial p}\right)_T$	$\left(\frac{1}{\beta\phi}\right)\left(\frac{\partial n}{\partial p}\right)_\phi$	$\frac{1}{\beta T}\left(\frac{\partial n}{\partial p}\right)_T$
	$^\circ C$								
CCl_4	25	1.45881	.469	.5320	.4882	.4588			
	35	1.45274	.418	.5326	.4815	.4527			
	45	1.44658	.446	.5151	.4747	.4465			
Benzene	25	1.49840	.395	.5879	.5319	.4984	.526	.522	.467
	35	1.49182	.503	.5785	.5246	.4918			.468
	45	1.48524	.559	.5691	.5173	.4852			.477
Water	2°	1.33438	.343	.3685	.3518	.3343			
	8°	1.33422	.364	.3683	.3516	.3342			
	23.1	1.3326		.3664	.3467	.3326	.325	.321	
	25	1.33292	.340	.3667	.3502	.3321			
	35	1.33170	.354	.3652	.3488	.3317			
	45	1.33024	.308	.3634	.3473	.3302			
	55	1.32855	.326	.3613	.3454	.3285			
Methyl Alcohol	22.8	1.3280		.3609	.3449	.328	.338	.329	
Carbon disulphide	22.6	1.6261		.7818	.6737	.6261	.6988	.7125	

Conclusion

The Eykman formula gives a value for $1/\beta\ (dn/dp)$ which is of the order of 6 to 12 percent lower than that given by the uncorrected Lorenz-Lorentz equation for the liquids studied, and which agree much better with the experimental values. For those liquids both the Eykman formula and the Gladstone-Dale relation give values which agree with the experimental values of Raman and Venkataraman to within 7 percent, the Eykman values being in general above, and the Gladstone-Dale values in general below, the experimental ones. Listed in Table II are the most probable values for $1/\beta\ (\partial n/\partial p)$. The accuracy of these values is certainly 10 percent. They are essentially mean values of all those found in the literature, weighted in the direction of the values given by Raman and Venkataraman since these appear to be most dependable. Also listed are the indices of refraction and the values obtained by using the Gladstone-Dale relation.

Table II.

Liquid	n	most probable $\frac{1}{\beta}\left(\frac{\partial n}{\partial p}\right)$	Gladstone Dale (n-1)
CCl_4	1.458	0.48	.458
Benzene	1.498	0.51	.498
Water	1.322	0.33	.332
Methyl Alcohol	1.328	0.33	.328

BIBLIOGRAPHY

1. L. Lorenz, Wied. Ann. 11, 70 (1880).

2. H. A. Lorentz, Wied. Ann. 9, 641 (1880).

3. M.J.F. Eykman, Rec. des Trav. Chim. 14, 177 (1895).

4. G. W. Willard, J. Acoust. Soc. Am. 12, 438 (1941).

5. V. Raman and K. S. Venkataraman, Proc. Roy. Soc. (London) 171, 137 (1939).

6. R. E. Gibson and J. F. Kincaid, J. Am. Chem. Soc. 60, 511 (1938).

7. R. Waxler, Private Communication.

DISTRIBUTION LIST FOR UNCLASSIFIED TECHNICAL REPORTS

Office of Naval Research (Code 468)
Department of the Navy
Washington 25, D. C. (2 copies)

Director
U. S. Naval Research Laboratory
Technical Information Division
Washington 25, D. C. (6 copies)

Director
U. S. Naval Research Laboratory
Sound Division
Washington 25, D. C. (1 copy)

Commanding Officer
Office of Naval Research Branch Office
The John Crerar Library Building
86 East Randolph Street
Chicago 1, Illinois (1 copy)

Commanding Officer
Office of Naval Research Branch Office
Box 39, Navy No. 100
FPO, New York (12 copies)

Armed Services Technical Information Agency
Arlington Hall Station
Arlington 12, Virginia (10 copies)

Commander
U. S. Naval Ordnance Laboratory
Acoustics Division
White Oak
Silver Spring, Maryland (1 copy)

Commanding Officer and Director
U. S. Navy Electronics Laboratory
San Diego 52, California (1 copy)

Director
U. S. Navy Underwater Sound Reference
Laboratory
Office of Naval Research
P. O. Box 8337
Orlando, Florida (1 copy)

Western Reserve University
Department of Chemistry
Cleveland, Ohio
(Attn: Dr. E. Yeager) (1 copy)

Commanding Officer and Director
U.S. Navy Underwater Sound Lab.
Fort Trumbull
New London, Connecticut (1 copy)

Commander
U. S. Naval Air Development Center
Johnsville, Pennsylvania (1 copy)

Director
National Bureau of Standards
Connecticut Ave. and Van Ness St.,N.W
Washington 25, D. C.
(Attn: Chief of Sound Section)
(1 copy)

Commanding Officer and Director
David Taylor Model Basin
Washington 7, D. C. (1 copy)

Superintendent
U. S. Navy Postgraduate School
Monterey, California
(Attn: Prof. L.E. Kinsler)(1 copy)

Commanding Officer
U. S. Navy Mine Defense Laboratory
Panama City, Florida (1 copy)

U. S. Naval Academy
Annapolis, Maryland
(Attn: Library) (1 copy)

Harvard University
Acoustics Laboratory
Division of Applied Science
Cambridge 38, Mass. (1 copy)

Brown University
Department of Physics
Providence 12, R. I. (1 copy)

Director
Ordnance Research Laboratory
Pennsylvania State University
University Park, Pa. (1 copy)

Defense Research Laboratory
University of Texas
Austin, Texas

University of California
Department of Physics
Los Angeles, California (1 copy)

University of California
Marine Physical Laboratory
Scripps Institution of Oceanography
San Diego 52, California (1 copy)

Bell Telephone Laboratories
Whippany, N. J. (1 copy)

Director
Columbia University
Hudson Laboratories
145 Palisades Street
Dobbs Ferry, N. Y. (1 copy)

Woods Hole Oceanographic Institute
Woods Hole, Massachusetts (1 copy)

Dr. J. R. Smithson
Electrical Engineering Department
U. S. Naval Academy
Annapolis, Maryland (1 copy)

Edwards Street Laboratory
Yale University
Box 1916 Yale Station
New Haven 11, Conn. (1 copy)

Lamont Geological Observatory
Columbia University
Torrey Cliffs
Palisades, N. Y. (1 copy)

The Catholic University of America
Department of Physics
Washington, D. C. (1 copy)

Massachusetts Institute of Technology
Laboratory of Electronics
Cambridge 39, Mass.
(Attn: Dr. U. Ingard) (1 copy)

Bureau of Naval Weapons
Code RU-222 (Oceanographer)
Washington 25, D. C. (1 copy)

Dr. George Hudson
Department of Physics
New York University
University Heights
New York 53, N. Y. (1 copy)

Bureau of Ships (Code 345)
Department of the Navy
Washington 25, D. C. (1 copy)

Bureau of Ships (Code 688)
Department of the Navy
Washington 25, D. C. (1 copy)

Bureau of Naval Weapons (RUDC)
Department of the Navy
Washington 25, D. C.

U. S. Navy SOFAR Station
APO No. 856, c/o Postmaster
New York, New York
(Attn: Mr. G.R. Hamilton)(1 copy)

John Carroll University
University Heights
Cleveland 18, Ohio
(Attn: E. F. Carome) (1 copy)

Edo Corporation
College Point, L. I., New York
(Attn: C. Loda) (1 copy)

Mr. Fred O. Briggson
ONR Resident Representative
University of Michigan
820 East Washington St.
Ann Arbor, Michigan (1 copy)

Naval Ordnance Test Station
Pasadena 8, California (1 copy)

Applied Physics Laboratory
University of Washington
Seattle, Washington (1 copy)

Dr. W. J. Fry
Biophysical Research Laboratory
University of Illinois
Urbana, Illinois (1 copy)

Institute for Defense Analyses
Communications Research Division
von Neumann Hall
Princeton, New Jersey (1 copy)

Dr. Alfred Weissler
Department of Chemistry
American University
Washington 16, D. C. (1 copy)

Dr. K. L. Zankel
Department of Physics
University of Oregon
Eugene, Oregon (1 copy)